

Implications of the latest XENON100 and cosmic ray antiproton data for isospin violating dark matter

Hong-Bo Jin^{*}, Sen Miao[†] and Yu-Feng Zhou[‡]

*State Key Laboratory of Theoretical Physics,
Kavli Institute for Theoretical Physics China,
Institute of Theoretical Physics, Chinese Academy of Sciences
Beijing, 100190, P.R. China*

Abstract

In the scenario of isospin violating dark matter (IVDM), the dark matter (DM) spin-independent couplings to protons and to neutrons are allowed to be different, which has been considered to relax the tensions between the results of DAMA, CoGeNT and XENON experiments. We explore the allowed values of DM-nucleon couplings favored and excluded by the current experiments under the assumption of IVDM. We find that the recently updated XENON100 result excludes the main part of the overlapping signal region between DAMA and CoGeNT. We also show that the possible tensions between some experiments such as that between DAMA and SIMPLE are unlikely to be affected by isospin violating interactions. In an effective operator approach, we investigate conservative upper bounds on the DM-quark couplings required by the IVDM scenario from the cosmic ray antiproton fluxes measured recently by BESS-Polar II and PAMELA, and that from the relic density. The results show that the relatively large couplings favored by DAMA and CoGeNT are tightly constrained, if the operators contribute to velocity-independent annihilation cross sections. For thermal relic DM, the upper bounds from the relic density can also be stringent.

^{*}Email: hbjin@itp.ac.cn

[†]Email: miaosen@itp.ac.cn

[‡]Email: yfzhou@itp.ac.cn

1 Introduction

It has been well established from astrophysical and cosmological observations that nearly 85% of the matter in the Universe consists of invisible dark matter (DM). So far the evidence of DM arise solely from its gravitational interactions. Popular DM candidates, such as the weakly interacting massive particles (WIMPs) can naturally reproduce the observed relic density through weak interactions with the standard model (SM) particles. This possibility has motivated numerous experiments to probe the direct or indirect signals of DM interacting with ordinary matter.

Some of the recent DM direct detection experiments such as DAMA [1–3], CoGeNT [4, 5] and CRESST-II [6] have reported events in excess of known backgrounds. The excess events, if interpreted in terms of DM particle elastic scattering off target nuclei, may imply light DM particles with mass around 8-10 GeV and scattering cross section around 10^{-40} cm². Other experiments such as CDMS-II [7,8], XENON10/100 [9,10], and SIMPLE [11] etc., have reported null results in the same DM mass range. The understanding of the backgrounds and systematic uncertainties in the current experiments still needs to be improved. At the moment, It is premature to draw a conclusion based on a single experimental result.

A commonly adopted assumption on interpreting the DM direct detection data is that in spin-independent scatterings the DM particle couplings to proton (f_p) and to neutron (f_n) are nearly the same, i.e. $f_n \approx f_p$, which makes it straight forward to extract the DM-nucleon scattering cross sections. However, in generic cases, the interactions may be isospin-violating [12–18]. In the scenario of isospin violating DM (IVDM), the DM particle couples to proton and neutron with different strengths, possible destructive interference between the two couplings can weaken the bounds from XENON10/100 and move the signal regions of DAMA and CoGeNT to be closer to each other [16,17]. In order to reconcile the data of DAMA, CoGeNT and XENON10/100, a large destructive interference corresponding to $f_n/f_p \approx -0.7$ is favored [16].

Recently, the XENON100 collaboration has reported updated results based on the exposure of 225 days with 34 kg fiducial mass [19]. Two events are observed with background expectation of 1.0 ± 0.2 events (0.79 ± 0.16 from gammas and $0.17^{+0.12}_{-0.07}$ from neutrons). The updated upper bound on the spin-independent scattering cross section is 2×10^{-45} cm² at 90% confidence level (CL) for a 55 GeV DM particle, which is improved by a factor of 3.5 in comparison with the previous result reported in 2011 [10]. For an 8 GeV DM particle, the limit is improved by a factor of five. Such a significant improvement may allow the XENON100 result to challenge the DAMA and GoGeNT results even in the scenario of IVDM.

As a consequence of $f_n/f_p \approx -0.7$, the absolute values $|f_{p,n}|$ have to be around two

order of magnitudes larger than that obtained under the assumption of IC interaction. At quark level, this means that the absolute DM couplings to the first generation u - and d -quarks must be enhanced by the same order of magnitudes. The scenario of IVDM with such light DM masses and relatively large couplings to light quarks can be tested in other processes in which there is no destructive interference. For instance, the light DM particles can be pair produced at the Large Hadron Collider (LHC) and the Tevatron with signals of a single jet/photon plus a large missing transverse energy, i.e. a mono-jet/mono-photon. The current null search results from LHC [20, 21] and Tevatron [22] can be used to impose constraints on the DM-quark couplings [23–26] and the IVDM [27].

As the inverse processes of DM production, light DM particles can annihilate into light-quark pairs in the galactic halo, which provides exotic sources of cosmic gamma rays, neutrinos and antiprotons. The annihilation processes occur at low velocities $v/c \approx \mathcal{O}(10^{-3})$ where c is the speed of light, which can be used to test the IVDM complementary to that at the LHC and Tevatron. For such low energy processes, the effective operator approach can be valid as long as the intermediate mediator particles are significantly heavier than the DM particle, but could be much lighter than the TeV scale (for recent discussions, see e.g. Refs. [24, 25, 28–31]). Possible constraints from the cosmic neutrinos and gamma ray on IVDM have been discussed in Refs. [32–34]. Recently the BESS-Polar II experiment has measured the antiproton flux in the energy range from 0.2 GeV to 3.5 GeV [35] which have higher precision compared with that from PAMELA [36] at low energies. The antiproton flux in this energy range can receive significant contributions from the annihilation of 10 GeV scale DM particles, provided that the annihilation cross section is not velocity suppressed. The constraints from BESS-Polar II data have been investigated recently for typical thermal WIMP using semi-analytical approach [37]. The constraints on the IVDM was briefly discussed in Ref. [34] which however did not provide a detailed analysis on the model parameters and uncertainties. In this work, we shall perform a more systematic analysis on implications of the recent cosmic ray antiproton flux data for IVDM, which is based on the fully numerical GALPROP approach. We shall compare several propagation models and aim at obtaining conservative upper bounds on the isospin-violating couplings.

For thermal relic DM, the same annihilation process also determines the DM relic density. By requiring that the calculated relic density from a single annihilation channel should not be smaller than the observed value $\Omega h^2 = 0.113 \pm 0.004$ [38], upper bounds on the DM couplings can be obtained. The bounds could be stringent if the annihilation is dominated by s -wave processes. For p -wave annihilation, although the cross section is velocity-suppressed, useful upper bounds can still be obtained as the typical relative velocity of DM particles is finite $v/c \approx 0.3$ at freeze out,

In this work, We first explore the values of DM-nucleon couplings favored by the current experiment under the assumption of IVDM for various target material and values of f_n/f_p . We find that the recently updated XENON100 result is able to rule out the main part of the marginally overlapping signal region between DAMA and CoGeNT unmodulated data for both the cases with and without considering the surface event rejection factors. We also show that the tensions between some group of experiments are unlikely to be affected by isospin violation, especially that between DAMA and SIMPLE. We adopt the effective operator approach to investigate the constraints from the antiproton flux data and the thermal relic density on the couplings between the IVDM and the SM light quarks. We calculate the antiproton flux using the numerical method implemented in the GALPROP code [39–42], and consider a number of propagation parameter configurations in order to obtain conservative upper bounds. The results show that the large and negative value $f_n/f_p = -0.7$ is severely constrained for the operators with velocity-independent annihilation cross sections, such as the fermionic DM with vector couplings and complex scalar DM with scalar couplings. For these operators we also find that the constraints from the cosmic antiproton flux are stronger than that from the thermal relic density. The relic density can provide useful constraint in the case where the operators contribute only to velocity suppressed annihilation cross sections. For the complex scalar DM with derivative couplings, we find that the IVDM is in some tension with the relic density.

This paper is organized as follows. In Section 2, we discuss the effect of IVDM on various target nuclei in different experiments and then explore the allowed DM couplings to nucleons and to light quarks. In Section 3, we list the effective operators relevant to the IVDM and the related interaction cross sections. In Section 4, we derive constraints on IVDM from the current cosmic ray antiproton data. In section 5 the constraints from the DM relic density is discussed. The numerical results are presented in Section 6 and the conclusions are given in Section 7.

2 Isospin violating dark matter

For a DM particle χ with mass m_χ elastically scattering off a target nucleus with atomic number Z and atomic mass number A , the recoil event rate $R = dN/dt$ is given by

$$R = N_T \left(\frac{\rho_0}{m_\chi} \right) \int dE_R \int_{v_{min}}^{v_{esc}} d^3v f(v) v \frac{d\sigma}{dE_R}, \quad (1)$$

where N_T is the total number of the target nuclei and ρ_0 is the local DM energy density which takes typical values in the range $0.2 - 0.56 \text{ GeV} \cdot \text{cm}^{-3}$ [43]. For a fixed recoil energy E_R , the required minimal velocity of the DM particle is $v_{min} = [m_A E_R / (2\mu_A^2)]^{1/2}$,

where m_A is the mass of the target nucleus and $\mu_A = (m_\chi m_A)/(m_\chi + m_A)$ is the DM-nucleus reduced mass. The maximal velocity is the escape velocity from our Galaxy at the position of the Solar system $v_{esc} \approx 600 \text{ km} \cdot \text{s}^{-1}$. The differential scattering cross section can be written as

$$\frac{d\sigma}{dE_R} = \frac{m_A F^2(E_R)}{2\mu_A^2 v^2} \sigma_0, \quad (2)$$

where $F(E_R)$ is the form factor of the nucleon. Here we have assumed that the form factors for proton and neutron are nearly identical, i.e., $F_p(E_R) \approx F_n(E_R) \equiv F(E_R)$. The quantity σ_0 can be understood as the total scattering cross section at the limit of zero-momentum transfer which is related to $f_{p(n)}$ through

$$\sigma_0 = \frac{\mu_A^2}{\pi} [Z f_p + (A - Z) f_n]^2. \quad (3)$$

Here it is assumed that the cross section is independent of the velocity of the DM particle. The cross section for the DM particle scattering off a free nucleon in term of $f_{p(n)}$ is

$$\sigma_{p(n)} = \frac{\mu_{p(n)}^2}{\pi} f_{p(n)}^2, \quad (4)$$

where $\mu_{p(n)}$ is the DM-proton (neutron) reduced mass. Under the assumption that the scattering is isospin conserving (IC), i.e., $f_n \approx f_p$, the total cross section σ_0 is independent of Z and only proportional to A^2 . One can define a cross section σ_p^{IC} which is the value of σ_p extracted from σ_0 under the assumption of IC interaction as

$$\sigma_p^{IC} \equiv \frac{\mu_p^2}{\mu_A^2 A^2} \sigma_0, \quad (5)$$

which is the quantity commonly reported by the experiments. In the generic case where $f_n \neq f_p$, the true value of σ_p will differ from σ_p^{IC} by a factor $F(f_n/f_p)$ which depends on the ratio f_n/f_p and the target material

$$\sigma_p = F(f_n/f_p) \sigma_p^{IC}. \quad (6)$$

Depending on the mass of the DM particle, for a given target material, for instance CaWO_4 used by CRESST-II experiment there could be multiple-target nuclei relevant to the nuclear recoil. If the target material consists of N kind of relevant nuclei with atomic numbers Z_α ($\alpha = 1, \dots, N$) and fractional number abundances κ_α , and for each nucleus Z_α there exists M type of isotopes found in nature with atomic mass number $A_{\alpha i}$ and fractional number abundance $\eta_{\alpha i}$ ($i = 1, \dots, M$), the expression of $F(f_n/f_p)$ can be explicitly written as

$$F(f_n/f_p) = \frac{\sum_{\alpha,i} \kappa_\alpha \eta_{\alpha i} \mu_{A_{\alpha i}}^2 A_{\alpha i}^2}{\sum_{\alpha,i} \kappa_\alpha \eta_{\alpha i} \mu_{A_{\alpha i}}^2 [Z_\alpha + (A_{\alpha i} - Z_\alpha) f_n/f_p]^2}, \quad (7)$$

where $\mu_{A_{\alpha i}}$ is the reduced mass for the DM and the nucleus with atomic mass number $A_{\alpha i}$. In the simplest case where the target consists of one kind of nucleus (Z, A), $F(f_n/f_p)$ takes the simple form

$$F(f_n/f_p) = \left[\frac{Z}{A} + \left(1 - \frac{Z}{A} \right) \frac{f_n}{f_p} \right]^{-2}. \quad (8)$$

It is evident that $F(f_n/f_p)$ approaches unity in the case of IC scattering. If $f_n/f_p < 0$ the interference between the contributions from proton and neutron scattering to the value of $F(f_n/f_p)$ will be destructive, which can lead to $F(f_n/f_p) \gg 1$. Thus it is possible that the value of σ_p can be a few order of magnitudes larger than σ_p^{IC} , provided a nearly complete cancellation between the two contributions.

For a given target material T , there is a particular value of f_n/f_p which corresponds to the maximal possible value of $F(f_n/f_p)$

$$\xi_T \equiv - \frac{\sum_{\alpha,i} \kappa_{\alpha} \eta_{\alpha i} \mu_{A_{\alpha i}}^2 (A_{\alpha i} - Z_{\alpha}) Z_{\alpha}}{\sum_{\alpha,i} \kappa_{\alpha} \eta_{\alpha i} \mu_{A_{\alpha i}}^2 (A_{\alpha i} - Z_{\alpha})^2}. \quad (9)$$

For a single nucleus target with atomic (mass) number $Z(A)$, it is simply given by $\xi_Z = -Z/(A - Z)$. The value of ξ_T varies with target material. In Tab. 1, we list the values of ξ_T for some typical material utilized by the current or future experiments.

	Xe	Ge	Si	Na(I)	Ca(W)O ₄	C ₂ ClF ₅	CsI	Ar
ξ_T	-0.70	-0.79	-1.0	-0.92(-0.73)	-1.0(-0.69)	-0.92	-0.71	-0.82

Table 1: Values of ξ_T for different target material. For NaI, the two values -0.92 and -0.73 correspond to the scattering off Na and NaI respectively. Similarly, for CaWO₄, the two values -1.0 and -0.69 corresponds to the scattering without and with tungsten nuclei respectively.

In Fig. 1, we plot the regions favored and excluded by the current experiments in the plane of $(f_p, f_n/f_p)$ for four different DM masses from 7.5 GeV to 9.0 GeV. The experimental results include: 90% CL upper bounds from CDMS-II Si and Ge [7,8], CRESST-II 2σ favored region for scattering without involving tungsten nucleus [6], DAMA 3σ favored region assuming Na scattering without considering the channeling effects [3], GoGeNT 90% favored region without considering the surface rejection correction factor [5], 90 % CL upper bound from SIMPLE [11], the 90% CL upper bound from XENON10 which is insensitive to scintillation efficiency [9] and the 90% CL upper bound from the XENON100 [19]. As it has been noticed previously at $f_n/f_p = -0.70 = \xi_{\text{Xe}}$, the DAMA- and CoGeNT-favored regions can overlap, the sensitivities of XENON10/100 are maximally reduced by two order of magnitudes. However, the DAMA- and CoGeNT favored

regions are only marginally consistent with the new XENON limit for $m_\chi = 7.5$ and 8.0 GeV. For $m_\chi = 8.5$ and 9.0 GeV, the overlapping regions start to disappear. The CRESST-II result favors a heavier DM particle. The allowed region by CRESST-II at 2σ can only be seen in the lower-right frame in Fig. 1 for $m_\chi = 9.0$ GeV, and is below the DAMA-favored region.

In Fig. 2, the allowed regions by the current experiments are shown in the (σ_p, m_χ) plane for $f_n/f_p = -0.70$. In the plot, we include the CoGeNT allowed regions at 90% and 99% CL with the surface event rejection correction factor taken from Ref. [44]. The DAMA-favored region at 90% CL is also shown [3]. When the corrections from the surface event rejection are taken into account, the GoGeNT-favored region moves towards larger DM mass and lower cross section. As it can be seen, for $f_n/f_p = -0.70$, the corrected GoGeNT-favored region corresponds to $m_\chi \approx 10$ GeV and $\sigma_p \approx 10^{-38}$ cm² which has marginal overlap with both DAMA- and CRESST-favored regions. Very recently, the CoGeNT has reported updated correction factors [45] which are a little bit higher than that used in Ref. [44], thus the GoGeNT-favored region may move closer to the signal region of DAMA.

As shown in Fig. 2, at $f_n/f_p = -0.70$, the overlapping region between GoGeNT and DAMA may still be consistent with the exclusion curve from the XENON100 2011 data [10]. However, If one considers the recently updated upper bounds from XENON100 [19], the main bulk of the overlapping region is excluded for both the GoGeNT results with and without surface event rejection corrections. Thus the recent XENON100 2012 result has a significant impact on the understanding of the nature of DM. It challenges the IVDM as a scenario to reconcile the results of DAMA, CoGeNT and XENON.

From Fig. 2, at $f_n/f_p = -0.70$, the overlapping region between DAMA and CoGeNT seems also to be excluded by the results of SIMPLE [11] and CDMS-II independently [7, 8]. Note that there exists controversies regarding the detector stability of SIMPLE experiments [46, 47], the recoil energy calibration of CDMS experiment [48] and the extrapolation of the measured scintillation efficiency to lower recoil energy in the previous XENON100 data analysis [49, 50]. The recently updated XENON100 result not only has considerably larger exposure and substantial reduction of background from ⁸⁵Kr, but also adopts a hard cut in S1 acceptance, which removes nearly all the event below the measured scintillation efficiency and makes the extrapolation to low recoil energy irrelevant.

If the ξ_T values of the target material used by two experiments are very close to each other, the tension between the two experimental results, if exists, is less affected by the effect of isospin violation. From Tab. 1 one finds that $\xi_{\text{Na}} \approx \xi_{\text{C}_2\text{ClF}_5} = -0.92$, $\xi_{\text{Xe}} \approx \xi_{\text{CsI}} \approx -0.7$ and $\xi_{\text{Si}} \approx \xi_{\text{Ca(W)O}_4} = -1.0$. Thus the tension between DAMA signal

from Na recoil and the upper bound from SIMPLE is unlikely to be alleviated by isospin violation, which can be clearly seen in Fig. 1. Similarly, if there exists contradictions between XENON and KIMS, CoGeNT and the Ar based experiments such as DarkSide, it can hardly be explained by isospin violating scattering. The SIMPLE result is also useful in comparing with the CRESST-II which utilizes Ca(W)O_4 which has $\xi_{\text{Ca(W)O}_4} = -1.0$. Obviously, for the experiments use the same target material, the possible tension between them cannot be relaxed by isospin violation, such as the tension between CoGeNT and CDMS-II, as both use germanium as target nucleus.

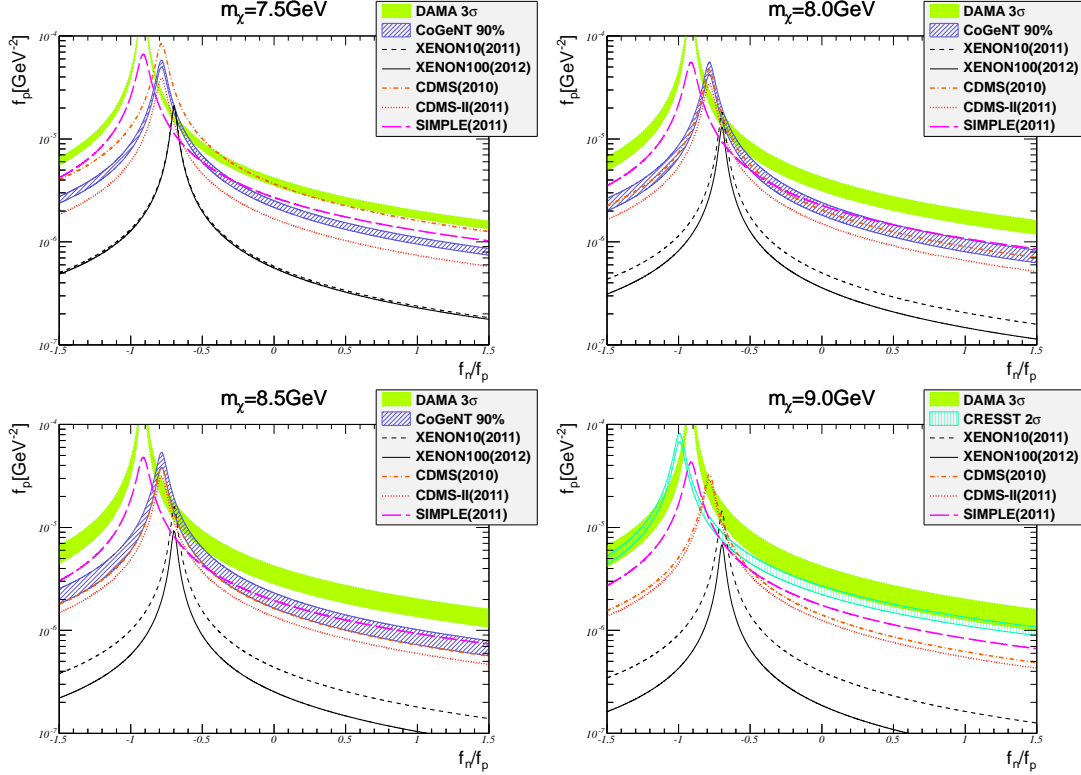


Figure 1: Favored regions and upper bounds in $(f_p, f_n/f_p)$ plane from current experiments DAMA [2], GoGeNT [5], XENON [9, 19], CDMS [7, 8] and SIMPLE [11] are also shown. Four panels corresponds to the four different mass of dark matter particle fixed at 7.5 GeV, 8.0 GeV, 8.5 GeV and 9.0 GeV respectively.

3 Effective interactions

We assume that the DM particles interact with the SM light quarks through some heavy mediator particles much heavier than the DM particle such that both the scattering and the annihilation processes can be effectively described by a set of high dimensional

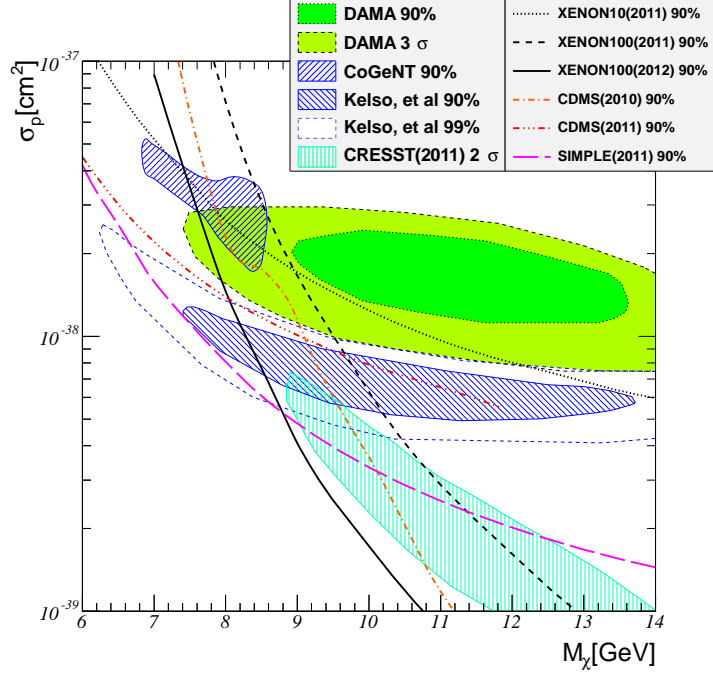


Figure 2: The favored regions and constraints in the (σ_p, m_χ) plane for various experiments for $f_n/f_p = -0.70$ such as DAMA [2], GoGeNT unmodulated data [5], CoGeNT unmodulated data with surface event rejection factors taken from Kelso, et al [44], CRESST-II [6], XENON10/100 [9, 19], CDMS [7, 8] and SIMPLE [11]. See text for explanation.

contact operators

$$\mathcal{L} = \sum_{i,q} a_{iq} \mathcal{O}_{iq} . \quad (10)$$

If the DM particles are Dirac fermions, the relevant operators arising from scalar or pseudoscalar interactions are given by

$$\mathcal{O}_{1q} = \bar{\chi}\chi\bar{q}q, \quad \mathcal{O}_{2q} = \bar{\chi}\gamma^5\chi\bar{q}q, \quad \mathcal{O}_{3q} = \bar{\chi}\chi\bar{q}\gamma^5q, \quad \mathcal{O}_{4q} = \bar{\chi}\gamma^5\chi\bar{q}\gamma^5q. \quad (11)$$

The operators from vector or axial-vector type interactions are

$$\mathcal{O}_{5q} = \bar{\chi}\gamma^\mu\chi\bar{q}\gamma_\mu q, \quad \mathcal{O}_{6q} = \bar{\chi}\gamma^\mu\gamma^5\chi\bar{q}\gamma_\mu q, \quad \mathcal{O}_{7q} = \bar{\chi}\gamma^\mu\chi\bar{q}\gamma_\mu\gamma^5q, \quad \mathcal{O}_{8q} = \bar{\chi}\gamma^\mu\gamma^5\chi\bar{q}\gamma_\mu\gamma^5q, \quad (12)$$

and the ones from the tensor interactions are

$$\mathcal{O}_{9q} = \bar{\chi}\sigma^{\mu\nu}\chi\bar{q}\sigma_{\mu\nu}q, \quad \mathcal{O}_{10q} = \bar{\chi}\sigma^{\mu\nu}\gamma^5\chi\bar{q}\sigma_{\mu\nu}q. \quad (13)$$

If the DM particles are Majorana particles the vector and tensor operators are vanishing. Among these operators only \mathcal{O}_{1q} and \mathcal{O}_{5q} contribute to spin-independent scattering

cross sections at low velocities. The scattering cross sections induced by the operators \mathcal{O}_{2q} and \mathcal{O}_{6q} are velocity suppressed. The operators \mathcal{O}_{7q} and \mathcal{O}_{8q} contribute only to spin-dependent scattering cross section, and the nucleus matrix elements for the operators \mathcal{O}_{3q} , \mathcal{O}_{4q} , \mathcal{O}_{9q} and \mathcal{O}_{10q} are either vanishing or negligible. The DM annihilation into quarks through \mathcal{O}_{1q} is a p -wave process, which is velocity suppressed. It does not contribute to the cosmic antiproton flux, but still contributes to the DM relic density as p -wave processes is non-negligible at freeze out.

Similarly, for DM being a complex scalar ϕ , possible operators are

$$\mathcal{O}_{11} = 2m_\phi(\phi^*\phi)\bar{q}q, \quad \mathcal{O}_{12} = 2m_\phi(\phi^*\phi)\bar{q}\gamma^5q, \quad \mathcal{O}_{13} = (\phi^*\overleftrightarrow{\partial}_\mu\phi)\bar{q}\gamma^\mu q, \quad \mathcal{O}_{14} = (\phi^*\overleftrightarrow{\partial}_\mu\phi)\bar{q}\gamma^\mu\gamma^5q. \quad (14)$$

Among those only \mathcal{O}_{11} and \mathcal{O}_{13} contribute to the spin-independent scatterings. The DM annihilations through operator \mathcal{O}_{13} are p -wave processes.

The fermionic or scalar DM may couple to gluons through the operators $\bar{\chi}\chi G_{\mu\nu}G^{\mu\nu}$, $\bar{\chi}\gamma^5\chi G_{\mu\nu}G^{\mu\nu}$, $\bar{\chi}\chi G_{\mu\nu}\tilde{G}^{\mu\nu}$ and $\bar{\chi}\gamma^5\chi G_{\mu\nu}\tilde{G}^{\mu\nu}$. We do not consider these operators as they do not contribute to isospin violating scatterings. In summary, we only consider the four operators

$$\mathcal{O}_{1q}, \quad \mathcal{O}_{5q}, \quad \mathcal{O}_{11q}, \quad \text{and} \quad \mathcal{O}_{13q},$$

which are relevant to IVDM.

The DM couplings to nucleons $f_{p,n}$ can be expressed in terms of the DM couplings to quarks a_{iq} as follows

$$f_{p(n)} = \sum_q B_{iq}^{p(n)} a_{iq}. \quad (15)$$

For the Dirac DM with scalar interaction $a_{1q}\bar{\chi}\chi\bar{q}q$, one has $B_{1q}^{p(n)} = f_{Tq}^{p(n)} m_{p(n)}/m_q$ for $q = u, d, s$ and $B_{1q}^{p(n)} = (2/27)f_{TG}^{p(n)} m_{p(n)}/m_q$ for $q = c, b, t$, where $f_{Tq}^{p(n)}$ is the DM coupling to light quarks obtained from the σ -term $\langle N|m_q\bar{q}q|N\rangle = f_{Tq}^N M_N$, and $f_{TG}^{p(n)} = 1 - \sum_{q=u,d,s} f_{Tq}^{p(n)}$. In numerical calculations we take $f_{Tu}^p = 0.020 \pm 0.004$, $f_{Td}^p = 0.026 \pm 0.005$, $f_{Ts}^p = 0.118 \pm 0.062$, $f_{Tu}^n = 0.014 \pm 0.003$, $f_{Td}^n = 0.036 \pm 0.008$ and $f_{Ts}^n = 0.118 \pm 0.062$ [51]. Using the following quark masses: $m_d = 0.005$ GeV, $m_u/m_d = 0.55$, $m_s = 0.095$ GeV, $m_c = 1.25$ GeV, $m_b = 4.2$ GeV and $m_t = 172.3$ GeV, we obtain the values of B_{iq} :

$$\begin{aligned} B_{1u}^p &\simeq B_{1d}^n \simeq 6.8, \quad B_{1d}^p \simeq B_{1u}^n \simeq 4.8, \\ B_{1s}^{p,n} &\simeq 1.2, \quad B_{1c}^{p,n} \simeq 0.05, \quad B_{1b}^{p,n} \simeq 1.5 \times 10^{-2}, \quad \text{and} \quad B_{1t}^{p,n} \simeq 3.5 \times 10^{-4}. \end{aligned} \quad (16)$$

In order to maximize the isospin violating effect, the coefficients $B_{1s,1c,1b,1t}^{p,n}$ must be strongly suppressed. Assuming that the DM-nucleon couplings are dominated by the

DM couplings to the first generation quarks, the ratio f_n/f_p is given by

$$\frac{f_n}{f_p} \approx \frac{B_{1u}^n a_{1u} + B_{1d}^n a_{1d}}{B_{1u}^p a_{1u} + B_{1d}^p a_{1d}}. \quad (17)$$

The value of $f_n/f_p = -0.7$ can be translated into $a_{1d}/a_{1u} = -0.93$ at quark level. This value is the same for complex scalar DM. For operator \mathcal{O}_{5q} one simply has $B_{5u}^{p(n)} = 2(1)$ and $B_{5d}^{p(n)} = 1(2)$, and $B_q^{p(n)} = 0$ for $q = c, s, t, b$.

$$\frac{f_n}{f_p} = \frac{a_{5u} + 2a_{5d}}{2a_{5u} + a_{5d}}. \quad (18)$$

Thus for $f_n/f_p = -0.7$, one finds $a_{5d}/a_{5u} = -0.89$. The cross section for DM annihilating into quarks induced by the relevant operators are given by

$$\begin{aligned} \sigma_{1q} v_{\text{rel}} (\bar{\chi}\chi \rightarrow \bar{q}q) &= \frac{N_C m_\chi^2}{2\pi} a_{1q}^2 v_{\text{rel}}^2, \\ \sigma_{5q} v_{\text{rel}} (\bar{\chi}\chi \rightarrow \bar{q}q) &= \frac{N_C m_\chi^2}{\pi} a_{5q}^2, \\ \sigma_{11q} v_{\text{rel}} (\bar{\phi}\phi \rightarrow \bar{q}q) &= \frac{N_C m_\phi^2}{\pi} a_{11q}^2, \\ \sigma_{13q} v_{\text{rel}} (\bar{\phi}\phi \rightarrow \bar{q}q) &= \frac{2N_C m_\phi^2}{3\pi} a_{13q}^2 v_{\text{rel}}^2, \end{aligned} \quad (19)$$

where $N_C = 3$ is the number of color and v_{rel} is the relative velocity of annihilating DM particles. For s -wave annihilation, the thermally averaged value of the cross section multiplied by velocity $\langle \sigma v_{\text{rel}} \rangle$ is the same as σv_{rel} .

4 Cosmic antiproton flux

Annihilation or decay of light DM particles in the galactic halo can contribute to exotic primary sources of the low energy cosmic ray antiprotons, which can be probed or constrained by the current satellite- and balloon-borne experiments such as PAMELA and BESS-polar II, etc.. The predicted antiproton flux from DM annihilation depends on models of the cosmic-ray transportation, the distribution of Galactic gas, radiation field and magnetic field, etc.. It also depends on the particle and nuclear interaction cross sections.

In this work, we use the numerical code GALPROP [39–42, 52] which utilizes realistic astronomical information on the distribution of interstellar gas and other data as input and consider various kinds of data including primary and secondary nuclei, electrons and positrons, γ -rays, synchrotron and radiation etc. in a self-consistent way. Other

approaches based on simplified assumptions on the Galactic gas distribution which allows for fast analytic solutions can be found in Refs. [53–56]. In the GALPROP approach, we consider several diffusion models (parameter configurations). The different results between the models can be regarded as an estimate of theoretical uncertainties.

In the diffusion models of cosmic ray propagation, the Galactic halo where diffusion occurs is parameterized by a cylinder with half height Z_h and radius $R = 20 - 30$ kpc. The densities of cosmic ray particles are vanishing at the boundary of the halo. The processes of energy losses, reacceleration and annihilation take place in the Galactic disc. The source terms for the secondary cosmic rays are also confined within the disc. The diffusion equation for the cosmic ray particle is given by

$$\begin{aligned} \frac{\partial \psi}{\partial t} = & \nabla(D_{xx} \nabla \psi - \mathbf{V}_c \psi) + \frac{\partial}{\partial p} p^2 D_{pp} \frac{\partial}{\partial p} \frac{1}{p^2} \psi - \frac{\partial}{\partial p} \left[\dot{p} \psi - \frac{p}{3} (\nabla \cdot \mathbf{V}_c) \psi \right] \\ & - \frac{1}{\tau_f} \psi - \frac{1}{\tau_r} \psi + q(\mathbf{r}, p), \end{aligned} \quad (20)$$

where $\psi(\mathbf{r}, p, t)$ is the number density per unit of total particle momentum which is related to the phase space density $f(\mathbf{r}, p, t)$ as $\psi(\mathbf{r}, p, t) = 4\pi p^2 f(\mathbf{r}, p, t)$. For steady-state diffusion, it is assumed that $\partial \psi / \partial t = 0$. The spatial diffusion coefficient D_{xx} is parameterized as

$$D_{xx} = \beta D_0 \left(\frac{\rho}{\rho_0} \right)^\delta, \quad (21)$$

where $\rho = p/(Ze)$ is the rigidity of cosmic ray particle and δ is the power spectral index which may take different values δ_1 or δ_2 when ρ is below or above the reference rigidity ρ_0 . D_0 is a normalization constant, and $\beta = v/c$ is the velocity of the cosmic ray particle. The values of D_0 and δ are determined from the measurements of the fluxes of other cosmic ray species such as the ratio of Boron to Carbon (B/C) and of isotopes $^{10}\text{Be}/^9\text{Be}$. The convection term is related to the drift of antiproton from the Galactic disc due to the Galactic wind. The direction of the wind is usually assumed to be along the z -direction which is perpendicular to the galactic disc and is a constant $\mathbf{V}_C = [2\theta(z) - 1]V_c$. The diffusion in momentum space is described by the reacceleration parameter D_{pp} which is related to the Alfvén speed V_a of the disturbances in the hydrodynamical plasma as

$$D_{pp} = \frac{4V_a^2 p^2}{3D_{xx} \delta (4 - \delta^2) (4 - \delta) w}, \quad (22)$$

where w stands for the level of turbulence which can be taken as $w = 1$ as D_{pp} depends only on the combination V_a^2/w . \dot{p} is related to the momentum loss rate, τ_f and τ_r are the time scale for fragmentation and radioactive decay respectively.

The sources of the primary particles are chosen to reproduce the cosmic-ray distribution determined by the EGRET γ -ray data. The injection spectrum of nuclei is assumed to have a broken power law behavior $dq(p)/dp \approx \rho^{-\gamma}$, with $\gamma = \gamma_1(\gamma_2)$ for the rigidity ρ below (above) a reference rigidity ρ_s . The secondary source is given in terms of the distributions of the primary particles $\psi(\mathbf{r}, p)$ and the distribution of the interstellar medium (ISM)

$$q(\mathbf{r}, p) = \beta c \psi_{prim}(\mathbf{r}, p) [\sigma_H(p) n_H(\mathbf{r}) + \sigma_{He} n_{He}(\mathbf{r})], \quad (23)$$

where $n_H(\mathbf{r})$ and $n_{He}(\mathbf{r})$ are the number densities of interstellar hydrogen and helium respectively. σ_H and σ_{He} are the cross sections for the generation of the secondary particles from the interactions with H and He. The detailed calculations of the cross sections and the distribution of interstellar gas can be found in Ref. [40] and references therein.

Thus the whole diffusion process depends on a number of parameters: R , Z_h , ρ_0 , D_0 , δ_1/δ_2 , V_c , V_a , ρ_s and γ_1/γ_2 . There exists degeneracies in the determination of the diffusion parameters from B/C. In general, increasing the diffusion half-height Z_h can be compensated by the increase of the diffusion constant D_0 , which leads to significant uncertainties in the predictions of antiproton flux from DM annihilation as the flux depends strongly on Z_h . The recently updated analysis based on Markov Chain Monte Carlo fits to the astrophysical data show that Z_h should be around 4–7 kpc [56, 57]. In order to obtain a conservative upper bounds we choose $Z_h \approx 4$ kpc in our analysis.

We consider several typical propagation models in GALPROP, and focus on the models with the secondary antiproton background below than the current data, which leaves room for DM contribution and results in conservative upper bounds. The first one is the plain diffusion model (referred to as “Plain”) in which there is no reacceleration term [42]. The second one is the conventional model (referred to as “Conventional”) with reacceleration included [41, 42]. The last one (referred to as “Global-Fit”) is the model from a global fit to the relevant astrophysical observables using Markov-Chain Monte Carlo method [57]. The main parameters of the three models are listed in Tab. 2. Note that in the three models the convection is not considered, as the inclusion of conversion term leads to problems in reproducing the spectrum of B/C and discontinuity in the propagation across the Galactic disc in GALPROP [42].

The primary source term from the DM annihilation has the form

$$q(\mathbf{r}) = \eta n(\mathbf{r})^2 \langle \sigma v_{rel} \rangle \frac{dN}{dp}, \quad (24)$$

where $n(\mathbf{r}) = \rho(\mathbf{r})/m_\chi$, $\eta = 1/2(1/4)$ if the DM particle is (not) its own antiparticle and dN/dp is the injection spectrum per DM annihilation. For the DM profile we took the

model	$R(\text{kpc})$	$Z_h(\text{kpc})$	D_0	ρ_0	δ_1/δ_2	$V_a(\text{km/s})$	ρ_s	γ_1/γ_2
Plain	30	4.0	2.2	3	0/0.60	0	40	2.30/2.15
Conventional	20	4.0	5.75	4	0.34/0.34	36	9	1.82/2.36
Global-Fit	20	3.9	6.59	4	0.3/0.3	39.2	10	1.91/2.40

Table 2: Propagation parameters in the “Plain” [42], “Conventional” [41, 42] and “Global-Fit” [57] models used in the GALPROP code. D_0 is in units of $10^{28}\text{cm}^2 \cdot \text{s}^{-1}$, the break rigidities ρ_0 and ρ_s are in units of GV.

isothermal profile [58]

$$\rho(\mathbf{r}) = \rho_0 \left(\frac{r_\odot^2 + R_s^2}{r^2 + R_s^2} \right), \quad (25)$$

where $r_\odot = 8.5$ kpc is the distance of Solar system from the galactic center, $R_s = 2.8$ kpc and the local density is taken to be $\rho_0 = 0.3 \text{ GeV cm}^{-3}$. The choice of isothermal profile and the local density is again to achieve a conservative estimate of the antiproton flux, if the NFW profile is used, the predicted flux will be enhanced roughly by at most 70%, thus more severe constraints are expected.

The total antiproton flux is related to the density function as

$$\Phi = \frac{v}{4\pi} \psi(p). \quad (26)$$

In the force-field approximation [59], the antiproton flux at the top of the atmosphere of the Earth $\Phi_{\bar{p}}^{TOA}$ which is measured by the experiments is related to the interstellar antiproton flux as

$$\Phi_{\bar{p}}^{TOA}(T_{TOA}) = \left(\frac{2m_p T_{TOA} + T_{TOA}^2}{2m_p T + T^2} \right) \Phi_{\bar{p}}(T), \quad (27)$$

where $T_{TOA} = T - \phi_F$ is the antiproton kinetic energy at the top of the atmosphere of the Earth. The BESS-Polar II data were taken in a period of lowest solar activity. We take $\phi_F = 0.5$ GV in numerical analysis.

5 DM thermal relic density

In the case where the DM particles are thermal relics, possible large couplings to light quarks may under predict the DM relic abundance in comparison with the observed value $\Omega h^2 = 0.113 \pm 0.004$ [38]. Thus the relic density can also impose upper bounds on the relevant couplings. Whereas the p -wave annihilation processes give no contribution to the antiproton flux, in the calculation of DM relic density, the p -wave annihilation

is nonnegligible as the typical relative velocity of DM particles is $v_{\text{rel}}/c \approx \mathcal{O}(0.3)$ at freeze out. The annihilation cross section times the relative velocity can be expressed as $\sigma v_{\text{rel}} = a + bv_{\text{rel}}^2$, where a and b are coefficients corresponding to the s -wave and p -wave contributions. The thermally averaged value at the time of freeze out has the form $\langle \sigma v_{\text{rel}} \rangle_f \simeq a + 6b/x_f$, where $x_f \equiv m_{DM}/T_f$ with T_f the decoupling temperature. The value of x_f can be estimated through the iterative solution of the equation [60]

$$x_f = \ln \left[C(C+2) \sqrt{\frac{45}{8}} \frac{g}{2\pi^3} \frac{M_{pl} m_{DM} (a + 6b/x_f)}{g_*^{1/2} x_f^{1/2}} \right], \quad (28)$$

where g is the number of degrees of freedom of the DM particle, g_* is the number of effective relativistic degrees of freedom of the thermal plasma and $M_{pl} = 1.22 \times 10^{19}$ GeV is the Planck energy scale. The constant C is determined by matching the semi-analytical solutions to the fully numerical solutions to the Boltzmann equation for the thermal evolution of particle number density. We take $C(C+2) = 1(2)$ for $s(p)$ -wave annihilation in numerical calculations. For light DM around 10 GeV, $g_* = 61.75$, we find $x_f \approx 22$. The relic abundance is approximately given by

$$\Omega h^2 \simeq \frac{1.07 \times 10^9 \text{ GeV}^{-1}}{M_{pl}} \frac{x_f}{\sqrt{g_*}} \frac{1}{a + 3bx_f}. \quad (29)$$

6 Results

We perform χ^2 analysis to obtain upper bounds on the DM isospin violating couplings to light quarks. Since within uncertainties the current BESS-Polar II and PAMELA data can be consistent with the secondary antiproton background, we consider one-side exclusion limit in which only the data points below the theoretical prediction are taken into account, namely we calculate the quantity $\chi^2 = \sum_i (\Phi_i^{\text{th}} - \Phi_i^{\text{exp}})^2 / \sigma_i^2$, (if $\Phi_i^{\text{th}} > \Phi_i^{\text{exp}}$), where Φ_i^{exp} are the measured fluxes with uncertainty σ_i and Φ_i^{th} are the theoretical predictions at kinetic energy T_i , and set upper bounds at 95% CL. The required χ^2 values for different degrees of freedom (d.o.f) are calculated from the standard χ^2 -distribution. For instance, the required χ^2 values are 64, 49.8, and 31.4 for d.o.f=47, 35, and 20 respectively. The upper bounds obtained in this manner is more conservative than that using the whole data set. The constraints from the relic density are also set at 95% CL. For the sake of simplicity, we consider one operator at a time and ignore interference between the operators.

For the operators contribute to s -wave annihilation which leads to velocity-independent annihilation cross sections, the relevant DM couplings to quarks are found to be tightly constrained by both the cosmic antiproton flux and the thermal relic density. In Fig. 3 the constraints on the coefficients a_{5q} for operator $\mathcal{O}_{5q} = \bar{\chi} \gamma^\mu \chi \bar{q} \gamma_\mu q$ are shown in the

$(a_{5u}, a_{5d}/a_{5u})$ plane. The mass of the Dirac DM particle is fixed at $m_\chi = 8$ GeV. The results show that the DAMA- and CoGeNT-favored regions are in tension with both the cosmic antiproton flux and the thermal relic density.

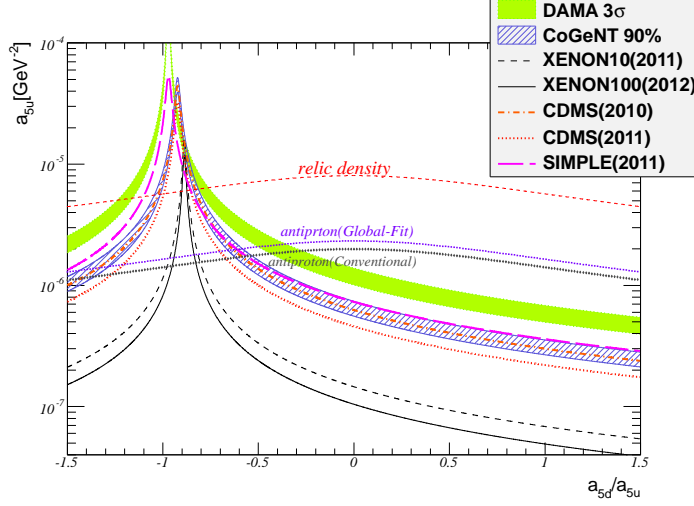


Figure 3: Upper bounds on the coefficient a_{5u} as a function of a_{5d}/a_{5u} at 95% CL from cosmic antiproton flux and DM relic density. The mass of DM particle is fixed at 8 GeV. The favored regions and exclusion contours from various experiments such as DAMA [2], GoGeNT [5], XENON [9, 19], CDMS [7, 8] and SIMPLE [11] are also shown.

At $a_{5d}/a_{5u} = -0.89$ which corresponds to $f_n/f_p = -0.70$, the DAMA and CoGeNT favored value is $a_{5u} \approx 1.6 \times 10^{-5} \text{ GeV}^{-2}$ corresponding to an annihilation cross section of $\langle \sigma v_{\text{rel}} \rangle \approx 3.4 \times 10^{-25} \text{ cm}^2$. As it can be seen in Fig. 4, for such a large cross section, the predicted antiproton flux is much higher than the current BESS-Polar II and PAMELA data and results in a huge $\chi^2/\text{d.o.f.} = 1.3 \times 10^6/35$ in the “Global-Fit” model and an even larger one in the “Conventional” model. The upper bound set by the antiproton data at 95% CL is $a_{5u} \leq 1.7 \times 10^{-6} \text{ GeV}^{-2}$ in the “Global-Fit” model at $a_{5d}/a_{5u} = -0.89$, which is about an order of magnitude lower and corresponds to an annihilation cross section $\langle \sigma v_{\text{rel}} \rangle \approx 3.7 \times 10^{-27} \text{ cm}^2$. The predicted antiproton fluxes are also shown in Fig. 4. In the two propagation models, the upper bound from the “Conventional” model is slightly stronger than that from the “Global-Fit” model. In Fig. 4, we also plot the antiproton background of “Plain” model which is already higher than the data. Thus the upper bounds from this propagation model are expected to be much stronger. Since we are interested in conservative upper bounds, we do not further investigate the constraints in this model. In Fig. 4, the upper bound from the relic density is $a_{5u} \leq 6.0 \times 10^{-6} \text{ GeV}^{-2}$ at $a_{5d}/a_{5u} = -0.89$, which is weaker than that from the antiproton flux but still in tension with the DAMA- and CoGeNT-favored value.

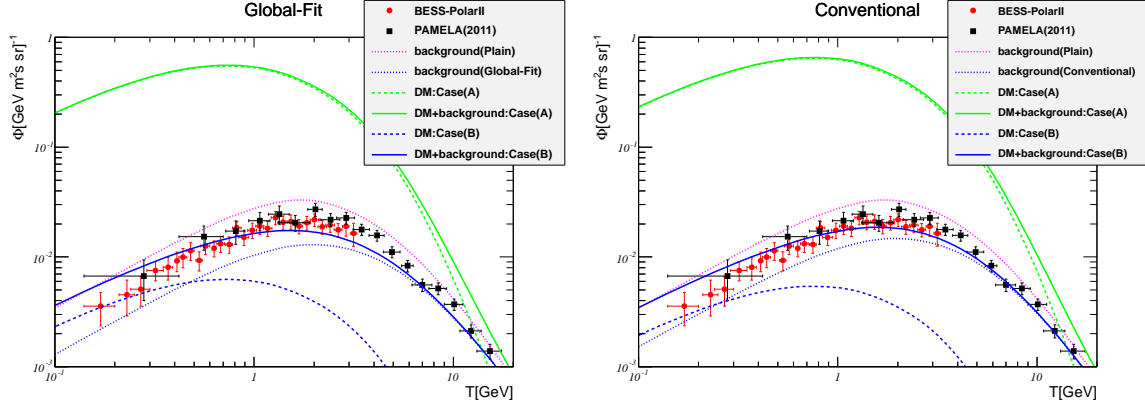


Figure 4: Left) predictions of cosmic antiproton spectra from DM annihilation induced by operator \mathcal{O}_{5q} in the “Global-Fit” propagation model. Two cases are considered: (A) For $a_{5u} = 1.6 \times 10^{-5} \text{ GeV}^{-2}$ which is favored by the DAMA and CoGeNT experiments. (B) For $a_{5u} = 1.7 \times 10^{-6} \text{ GeV}^{-2}$ which is the maximal value allowed by the cosmic antiproton data at 95% CL. The ratio a_{5d}/a_{5u} is fixed at -0.89 corresponding to $f_n/f_p = -0.70$ and the mass of DM particle is fixed at 8 GeV. The data of BESS-Polar II [35] and PAMELA [36] are also shown; right) Same as left), but for the “Conventional” model.

In Fig. 5 we show the constraints on the coefficients a_{11q} for operator $\mathcal{O}_{11} = 2m_\phi(\phi^*\phi)(\bar{q}q)$ in $(a_{11u}, a_{11d}/a_{11u})$ plane for the complex scalar DM mass fixed at $m_\phi = 8 \text{ GeV}$. For this operator, the DAMA- and CoGeNT-favored regions are still in tension with the antiproton flux. At $a_{11d}/a_{11u} = -0.93$ which corresponds to $f_n/f_p = -0.70$,

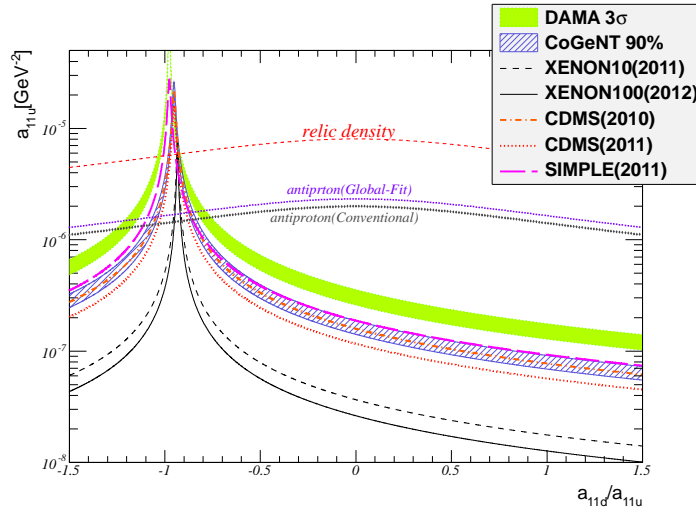


Figure 5: Same as Fig. 3, but for coefficients a_{11q} of operator $\mathcal{O}_{11} = 2m_\phi(\phi^*\phi)(\bar{q}q)$.

the DAMA- and CoGeNT-favored values is $a_{11u} \approx 7.9 \times 10^{-6} \text{ GeV}^2$, corresponding to an annihilation cross section of $\langle \sigma v_{\text{rel}} \rangle \approx 8.5 \times 10^{-26} \text{ cm}^2$. The predicted antiproton fluxes are shown in Fig. 6 which is again much higher than the current data. The upper bound set by the antiproton data is $a_{11u} \leq 1.7 \times 10^{-6} \text{ GeV}^2$ at $a_{11d}/a_{11u} = -0.93$. Compared with the case of \mathcal{O}_{5q} , the constraints on the coefficients of \mathcal{O}_{11q} are weaker, which is due to the fact that for the hadronic matrix element of scalar operator $\bar{q}q$ the B_{iq} factors are larger than that for vector operator $\bar{q}\gamma^\mu q$, which allows smaller a_{iq} for the same value of $f_{p,n}$ and results in smaller annihilation cross sections. The constraint from the thermal relic density is in tension with the DAMA- and CoGeNT-favored values.

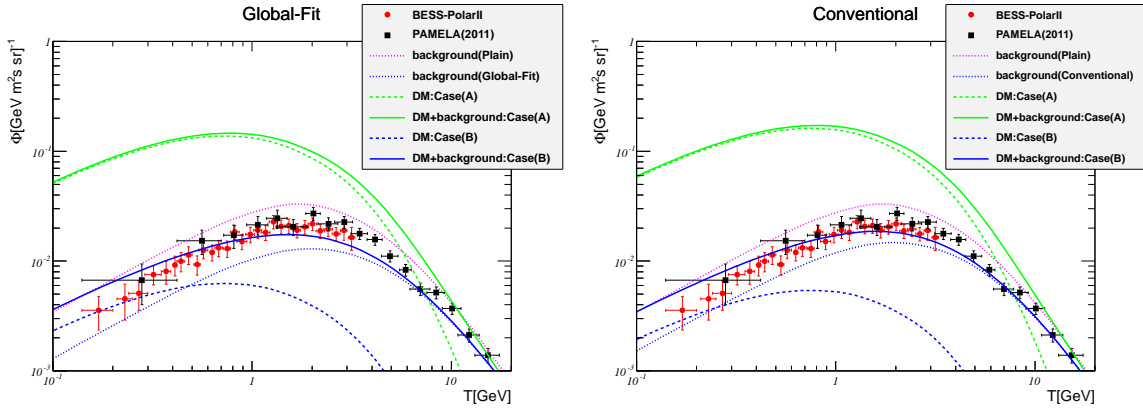


Figure 6: Left) predictions of cosmic antiproton spectra from DM annihilation induced by operator \mathcal{O}_{11q} in the “Global Fit” propagation model. Two cases are considered: (A) For $a_{11u} = 7.9 \times 10^{-6} \text{ GeV}^2$ which is favored by the DAMA and CoGeNT experiments. (B) For $a_{11u} = 1.7 \times 10^{-6} \text{ GeV}^2$ which is the maximal value allowed by the cosmic antiproton data at 95% CL. The ratio a_{11d}/a_{11u} is fixed at -0.93 corresponding to $f_n/f_p = -0.70$ and the mass of DM particle is 8 GeV. The data of BESS-Polar II [35] and PAMELA [36] are also shown; right) same as left), but for the “Conventional” model.

In Fig. 7, we show the favored regions and exclusion contours for operator \mathcal{O}_{5q} and \mathcal{O}_{11q} for the coefficients corresponding to $f_n/f_p = -0.70$ in (σ_p, m_{DM}) plane where m_{DM} is the mass of the Dirac or complex scalar DM particle in the range from 5 GeV to 15 GeV. For both operators, the DAMA- and CoGeNT-favored regions are far above the 95% CL bounds from the antiproton flux for all the values of DM mass in this range. The favored regions are also in tension with the thermal relic density, especially for \mathcal{O}_{5q} .

The operators $\mathcal{O}_{1q} = \bar{\chi}\chi\bar{q}q$ and $\mathcal{O}_{13q} = (\phi^* \overleftrightarrow{\partial}_\mu \phi)\bar{q}\gamma^\mu q$ contribute to p -wave annihilation with cross section proportional to v_{rel}^2 . Thus they do contribute very little to the cosmic

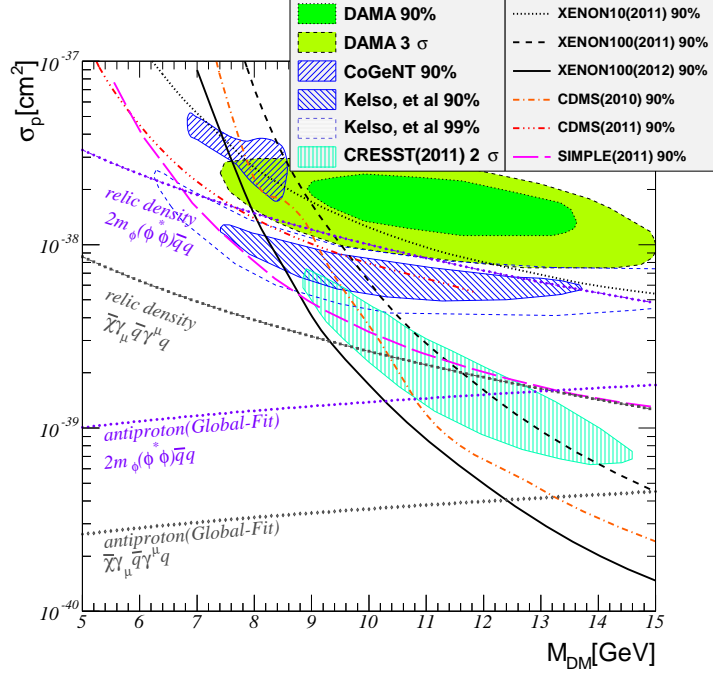


Figure 7: The favored regions and constraints in the (σ_p, m_{DM}) plane for operators \mathcal{O}_{5q} and \mathcal{O}_{11q} with the coefficients corresponding to $f_n/f_p = -0.7$.

antiproton flux. However, their contributions to the thermal relic density cannot be neglected, as at freeze out the relative velocity is finite. In Fig. 8, we show the constraints from relic density on the coefficients a_{1q} and a_{13q} . For the operator \mathcal{O}_{13q} one can see some tension between bounds set by the relic density and regions favored by DAMA and CoGeNT data. The constraint is not as stringent as that from the latest XENON100 data. For the operator \mathcal{O}_{1q} , the constraints from relic density is rather weak. The difference is again due to the different B_{iq} factors for these two type of interactions.

It is straight forward to extend the discussions to Majorana fermions and real scalars. For the particles being its own antiparticles the primary source of the antiproton will be enhanced by a factor of 2 in Eq. (24), which may lead to more stringent constraints.

7 Conclusions

In summary, we have investigated the allowed values of DM-nucleon couplings in the scenario of IVDM for various target nuclei used in DM direct detections. We find that the recently updated XENON100 result excludes the main part of the overlapping signal region between DAMA and CoGeNT. We have shown that whereas the effect of isospin violating scattering can relax the tensions between the data of DAMA, CoGeNT and

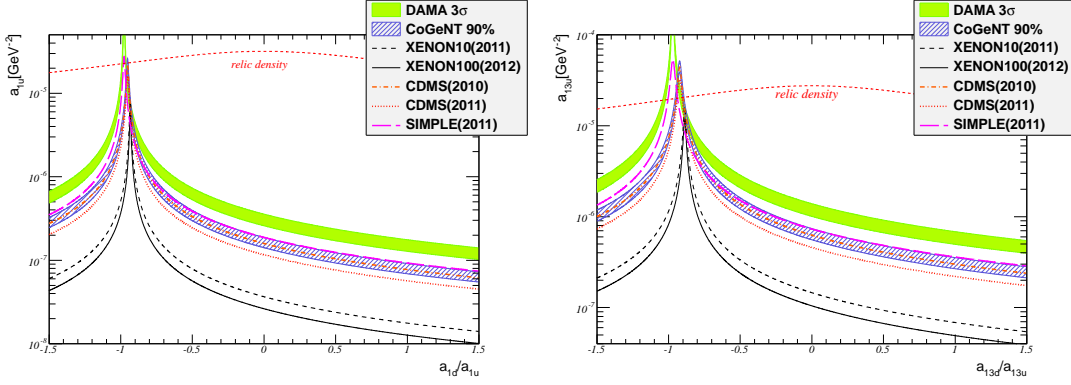


Figure 8: Left) constraints from thermal relic density on the coefficients a_{1q} of operator $\mathcal{O}_{1q} = \bar{\chi}\chi\bar{q}q$ in the $(a_{1u}, a_{1d}/a_{1u})$ plane. The mass of Dirac DM particle is fixed at $m_\chi = 8$ GeV. The favored regions and exclusion contours from various experiments are also shown; right) same as left), but for coefficients a_{13q} .

XENON, the possible disagreement between some group of experiments such as that between DAMA and SIMPLE are not likely to be affected for any value of f_n/f_p . In an effective operator approach, we have investigated the conservative constraints on the couplings between the IVDM and the SM light quarks from the recent cosmic ray antiproton data and that from the thermal relic density. Among the four operators relevant to IVDM \mathcal{O}_{1q} , \mathcal{O}_{5q} , \mathcal{O}_{11q} , \mathcal{O}_{13q} , the operators \mathcal{O}_{5q} and \mathcal{O}_{11q} are found to be tightly constrained by the antiproton data and \mathcal{O}_{13q} is constrained by the relic density. Only the operator \mathcal{O}_{1q} can survive both the constraints while contribute to large enough isospin violating interaction required by the current data of DAMA, CoGeNT and XENON.

The scenario of IVDM may be less constrained by the cosmic ray observations if the DM particles interact with SM particles only through some mediator particle ϕ such that the DM annihilation cannot be described by effective operators. For instance, if the mass of the light mediator m_ϕ is much smaller than that of the dark matter particle m_χ while still significantly larger than the typical recoil energy \sim keV, the effective operator approach is valid only for the elastic scattering but not for the annihilation. The cross section for DM annihilation will be suppressed by a factor of m_ϕ^4/m_χ^4 compared with the ordinary effective operator approach. The IVDM is also less constrained by the cosmic ray data if it is asymmetric.

Acknowledgments

We are grateful to Yue-Liang Wu for encouragement and helpful discussions. This work is supported in part by the National Basic Research Program of China (973 Program)

under Grants No. 2010CB833000; the National Nature Science Foundation of China (NSFC) under Grants No. 10975170, No. 10821504 and No. 10905084; and the Project of Knowledge Innovation Program (PKIP) of the Chinese Academy of Science.

References

- [1] **DAMA Collaboration** Collaboration, R. Bernabei *et. al.*, *First results from DAMA/LIBRA and the combined results with DAMA/NaI*, *Eur.Phys.J.* **C56** (2008) 333–355, [arXiv:0804.2741].
- [2] C. Savage, G. Gelmini, P. Gondolo, and K. Freese, *Compatibility of DAMA/LIBRA dark matter detection with other searches*, *JCAP* **0904** (2009) 010, [arXiv:0808.3607].
- [3] **DAMA** Collaboration, R. Bernabei *et. al.*, *New results from DAMA/LIBRA*, *Eur. Phys. J.* **C67** (2010) 39–49, [arXiv:1002.1028].
- [4] **CoGeNT** Collaboration, C. E. Aalseth *et. al.*, *Results from a Search for Light-Mass Dark Matter with a P- type Point Contact Germanium Detector*, *Phys. Rev. Lett.* **106** (2011) 131301, [arXiv:1002.4703].
- [5] C. E. Aalseth *et. al.*, *Search for an Annual Modulation in a P-type Point Contact Germanium Dark Matter Detector*, *Phys. Rev. Lett.* **107** (2011) 141301, [arXiv:1106.0650].
- [6] G. Angloher *et. al.*, *Results from 730 kg days of the CRESST-II Dark Matter Search*, arXiv:1109.0702.
- [7] **CDMS** Collaboration, D. S. Akerib *et. al.*, *Low-threshold analysis of CDMS shallow-site data*, *Phys. Rev.* **D82** (2010) 122004, [arXiv:1010.4290].
- [8] **CDMS-II** Collaboration, Z. Ahmed *et. al.*, *Results from a Low-Energy Analysis of the CDMS II Germanium Data*, *Phys. Rev. Lett.* **106** (2011) 131302, [arXiv:1011.2482].
- [9] **XENON10** Collaboration, J. Angle *et. al.*, *A search for light dark matter in XENON10 data*, *Phys. Rev. Lett.* **107** (2011) 051301, [arXiv:1104.3088].
- [10] **XENON100** Collaboration, E. Aprile *et. al.*, *Dark Matter Results from 100 Live Days of XENON100 Data*, *Phys. Rev. Lett.* **107** (2011) 131302, [arXiv:1104.2549].

- [11] M. Felizardo *et. al.*, *Final Analysis and Results of the Phase II SIMPLE Dark Matter Search*, [arXiv:1106.3014](#).
- [12] A. Kurylov and M. Kamionkowski, *Generalized analysis of weakly-interacting massive particle searches*, *Phys. Rev.* **D69** (2004) 063503, [[hep-ph/0307185](#)].
- [13] F. Giuliani, *Are direct search experiments sensitive to all spin- independent WIMP candidates?*, *Phys. Rev. Lett.* **95** (2005) 101301, [[hep-ph/0504157](#)].
- [14] A. L. Fitzpatrick, D. Hooper, and K. M. Zurek, *Implications of CoGeNT and DAMA for Light WIMP Dark Matter*, *Phys. Rev.* **D81** (2010) 115005, [[arXiv:1003.0014](#)].
- [15] S. Chang, J. Liu, A. Pierce, N. Weiner, and I. Yavin, *CoGeNT Interpretations*, *JCAP* **1008** (2010) 018, [[arXiv:1004.0697](#)].
- [16] J. L. Feng, J. Kumar, D. Marfatia, and D. Sanford, *Isospin-Violating Dark Matter*, *Phys. Lett.* **B703** (2011) 124–127, [[arXiv:1102.4331](#)].
- [17] M. T. Frandsen *et. al.*, *On the DAMA and CoGeNT Modulations*, *Phys. Rev.* **D84** (2011) 041301, [[arXiv:1105.3734](#)].
- [18] X.-G. He, B. Ren, and J. Tandean, *Hints of Standard Model Higgs Boson at the LHC and Light Dark Matter Searches*, *Phys.Rev.* **D85** (2012) 093019, [[arXiv:1112.6364](#)].
- [19] **XENON100 Collaboration** Collaboration, E. Aprile *et. al.*, *Dark Matter Results from 225 Live Days of XENON100 Data*, [arXiv:1207.5988](#).
- [20] **ATLAS Collaboration** Collaboration, G. Aad *et. al.*, *Search for New Phenomena in $t\bar{t}$ bar Events With Large Missing Transverse Momentum in Proton-Proton Collisions at $\sqrt{s} = 7$ TeV with the ATLAS Detector*, *Phys.Rev.Lett.* **108** (2012) 041805, [[arXiv:1109.4725](#)].
- [21] CMS Collaboration, (2012), CMS-PAS-EXO-11-059.
- [22] CDF Collaboration,
<http://www-cdf.fnal.gov/physics/exotic/r2a/20070322.monojet/public/ykk.html>.
- [23] Y. Bai, P. J. Fox, and R. Harnik, *The Tevatron at the Frontier of Dark Matter Direct Detection*, *JHEP* **1012** (2010) 048, [[arXiv:1005.3797](#)].

- [24] J. Goodman, M. Ibe, A. Rajaraman, W. Shepherd, T. M. Tait, *et. al.*, *Constraints on Light Majorana dark Matter from Colliders*, *Phys.Lett.* **B695** (2011) 185–188, [[arXiv:1005.1286](#)].
- [25] J. Goodman *et. al.*, *Constraints on Dark Matter from Colliders*, *Phys. Rev.* **D82** (2010) 116010, [[arXiv:1008.1783](#)].
- [26] M. T. Frandsen, F. Kahlhoefer, A. Preston, S. Sarkar, and K. Schmidt-Hoberg, *LHC and Tevatron bounds on the dark matter direct detection cross-section for vector mediators*, [arXiv:1204.3839](#).
- [27] A. Rajaraman, W. Shepherd, T. M. P. Tait, and A. M. Wijangco, *LHC Bounds on Interactions of Dark Matter*, *Phys. Rev.* **D84** (2011) 095013, [[arXiv:1108.1196](#)].
- [28] J. Goodman, M. Ibe, A. Rajaraman, W. Shepherd, T. M. Tait, *et. al.*, *Gamma Ray Line Constraints on Effective Theories of Dark Matter*, *Nucl.Phys.* **B844** (2011) 55–68, [[arXiv:1009.0008](#)].
- [29] W.-Y. Keung, I. Low, and G. Shaughnessy, *When CoGeNT met PAMELA*, *Phys.Rev.* **D82** (2010) 115019, [[arXiv:1010.1774](#)].
- [30] K. Cheung, P.-Y. Tseng, and T.-C. Yuan, *Cosmic Antiproton Constraints on Effective Interactions of the Dark Matter*, *JCAP* **1101** (2011) 004, [[arXiv:1011.2310](#)].
- [31] X. Gao, Z. Kang, and T. Li, *Light Dark Matter Models with Isospin Violation*, [arXiv:1107.3529](#).
- [32] J. Kumar, J. G. Learned, M. Sakai, and S. Smith, *Dark Matter Detection With Electron Neutrinos in Liquid Scintillation Detectors*, *Phys.Rev.* **D84** (2011) 036007, [[arXiv:1103.3270](#)].
- [33] S.-L. Chen and Y. Zhang, *Isospin-Violating Dark Matter and Neutrinos From the Sun*, *Phys.Rev.* **D84** (2011) 031301, [[arXiv:1106.4044](#)].
- [34] J. Kumar, D. Sanford, and L. E. Strigari, *New Constraints on Isospin-Violating Dark Matter*, *Phys.Rev.* **D85** (2012) 081301, [[arXiv:1112.4849](#)].
- [35] K. Abe *et. al.*, *Measurement of the cosmic-ray antiproton spectrum at solar minimum with a long-duration balloon flight over Antarctica*, *Phys. Rev. Lett.* **108** (2012) 051102, [[arXiv:1107.6000](#)].

- [36] **PAMELA Collaboration** Collaboration, O. Adriani *et. al.*, *The cosmic-ray electron flux measured by the PAMELA experiment between 1 and 625 GeV*, *Phys.Rev.Lett.* **106** (2011) 201101, [arXiv:1103.2880].
- [37] R. Kappl and M. W. Winkler, *Dark Matter after BESS-Polar II*, arXiv:1110.4376.
- [38] **WMAP Collaboration** Collaboration, E. Komatsu *et. al.*, *Seven-Year Wilkinson Microwave Anisotropy Probe (WMAP) Observations: Cosmological Interpretation*, *Astrophys.J.Suppl.* **192** (2011) 18, [arXiv:1001.4538].
- [39] A. Strong and I. Moskalenko, *Propagation of cosmic-ray nucleons in the galaxy*, *Astrophys.J.* **509** (1998) 212–228, [astro-ph/9807150].
- [40] I. V. Moskalenko, A. W. Strong, J. F. Ormes, and M. S. Potgieter, *Secondary anti-protons and propagation of cosmic rays in the galaxy and heliosphere*, *Astrophys.J.* **565** (2002) 280–296, [astro-ph/0106567].
- [41] A. Strong and I. Moskalenko, *Models for galactic cosmic ray propagation*, *Adv.Space Res.* **27** (2001) 717–726, [astro-ph/0101068].
- [42] V. Ptuskin, I. V. Moskalenko, F. Jones, A. Strong, and V. Zirakashvili, *Dissipation of magnetohydrodynamic waves on energetic particles: impact on interstellar turbulence and cosmic ray transport*, *Astrophys.J.* **642** (2006) 902–916, [astro-ph/0510335].
- [43] F. Iocco, M. Pato, G. Bertone, and P. Jetzer, *Dark Matter distribution in the Milky Way: microlensing and dynamical constraints*, *JCAP* **1111** (2011) 029, [arXiv:1107.5810].
- [44] C. Kelso, D. Hooper, and M. R. Buckley, *Toward A Consistent Picture For CRESST, CoGeNT and DAMA*, *Phys.Rev.* **D85** (2012) 043515, [arXiv:1110.5338].
- [45] **CoGeNT Collaboration** Collaboration, C. Aalseth *et. al.*, *CoGeNT: A Search for Low-Mass Dark Matter using p-type Point Contact Germanium Detectors*, arXiv:1208.5737.
- [46] J. Collar, *Comments on 'Final Analysis and Results of the Phase II SIMPLE Dark Matter Search'*, arXiv:1106.3559.
- [47] **SIMPLE Collaboration** Collaboration, *Reply to arXiv:1106.3559 by J.I. Collar*, arXiv:1107.1515.

- [48] J. Collar, *A comparison between the low-energy spectra from CoGeNT and CDMS*, [arXiv:1103.3481](#).
- [49] J. Collar and D. McKinsey, *Comments on 'First Dark Matter Results from the XENON100 Experiment'*, [arXiv:1005.0838](#).
- [50] **XENON100 Collaboration** Collaboration, *Reply to the Comments on the XENON100 First Dark Matter Results*, [arXiv:1005.2615](#).
- [51] J. R. Ellis, A. Ferstl, and K. A. Olive, *Re-evaluation of the elastic scattering of supersymmetric dark matter*, *Phys. Lett.* **B481** (2000) 304–314, [[hep-ph/0001005](#)].
- [52] I. V. Moskalenko, A. Strong, S. Mashnik, and J. Ormes, *Challenging cosmic ray propagation with antiprotons. Evidence for a fresh nuclei component?*, *Astrophys.J.* **586** (2003) 1050–1066, [[astro-ph/0210480](#)].
- [53] F. Donato, D. Maurin, P. Salati, A. Barrau, G. Boudoul, *et. al.*, *Anti-protons from spallations of cosmic rays on interstellar matter*, *Astrophys.J.* **563** (2001) 172–184, [[astro-ph/0103150](#)].
- [54] D. Maurin, R. Taillet, F. Donato, P. Salati, A. Barrau, *et. al.*, *Galactic cosmic ray nuclei as a tool for astroparticle physics*, [astro-ph/0212111](#).
- [55] F. Donato, N. Fornengo, D. Maurin, and P. Salati, *Antiprotons in cosmic rays from neutralino annihilation*, *Phys.Rev.* **D69** (2004) 063501, [[astro-ph/0306207](#)].
- [56] A. Putze, L. Derome, and D. Maurin, *A Markov Chain Monte Carlo technique to sample transport and source parameters of Galactic cosmic rays: II. Results for the diffusion model combining B/C and radioactive nuclei*, *Astron.Astrophys.* **516** (2010) A66, [[arXiv:1001.0551](#)].
- [57] R. Trotta, G. Johannesson, I. Moskalenko, T. Porter, R. R. de Austri, *et. al.*, *Constraints on cosmic-ray propagation models from a global Bayesian analysis*, *Astrophys.J.* **729** (2011) 106, [[arXiv:1011.0037](#)].
- [58] L. Bergstrom, P. Ullio, and J. H. Buckley, *Observability of gamma-rays from dark matter neutralino annihilations in the Milky Way halo*, *Astropart.Phys.* **9** (1998) 137–162, [[astro-ph/9712318](#)].
- [59] L. J. Gleeson and W. I. Axford, *Solar Modulation of Galactic Cosmic Rays*, *Astrophys. J.* **154** (1968) 1011.

- [60] G. Bertone, D. Hooper, and J. Silk, *Particle dark matter: Evidence, candidates and constraints*, *Phys.Rept.* **405** (2005) 279–390, [[hep-ph/0404175](#)].